ELSEVIER

Journal of Alloys and Compounds 293–295 (1999) 569–582

Journal of ALLOYS AND COMPOUNDS

# The correlation between composition and electrochemical properties of metal hydride electrodes

J.J. Reilly*, G.D. Adzic, J.R. Johnson, T. Vogt, S. Mukerjee, J. McBreen

*Department of Applied Science, Brookhaven National Laboratory, Upton, NY 11973, USA*

**Abstract**

This paper is concerned with an overview of the properties of metal hydride electrodes used for battery applications. The emphasis is on the properties of $AB_5$ electrodes but others are treated as well. The review begins with a brief discussion of the pertinent chemistry of hydrogen in metals, the properties of intermetallic hydrides and their relation to electrochemical behavior. Systematic guidelines which permit the modification of such properties for electrochemical applications are discussed. The electrochemical behaviors of certain specific $AB_5$ alloy electrodes are covered in detail, emphasizing the effects of composition changes with respect to both the A and the B components. The consequences of electrode expansion and contraction with respect to hydride formation and decomposition are discussed quantitatively. Novel alloy compositions and phases are noted and evaluated. The attractive properties of cobalt-free, non-stoichiometric $AB_{5+x}$ electrodes are noted. 

*Keywords:* Metal hydride electrodes; MH/Ni batteries

## 1. Introduction

For many years the focus of research in H/metal systems was on the storage of hydrogen for use as a gaseous fuel. In this connection an excellent overview of the behavior of $H_2$ gas/solid systems is given in a companion paper by Sandrock [1]. This paper will deal with electrochemical applications where a metal hydride ($MH_x$) electrode is used to replace the cadmium electrode in Ni/Cd batteries. The prime driving force for such replacement is the environmental problems associated with cadmium, but an additional benefit is also accrued; the higher energy density of the $MH_x$ electrode. This is the context in which we will discuss the electrochemical, thermodynamic and structural properties of metal hydrides.

## 2. Thermodynamics

Flanagan and Oates [2] have extensively reviewed the thermodynamics of intermetallic hydrides; also recommended are the classic work of Libowitz [3] and the comprehensive text of Muller et al. [4] which treats the properties of binary hydrides. The properties of a metal–hydrogen system can be conveniently summarized by a pressure–temperature–composition (PTC) diagram [1], which consists of a family of isotherms that relate the equilibrium pressure of hydrogen to the H content of the metal (see Fig. 1 for example). Initially the isotherm ascends steeply as hydrogen dissolves in the metal to form a solid solution; at low concentrations the behavior is ideal and obeys Sievert's Law, i.e.

$$H_{solid} = K_S P^{1/2} \quad (1)$$

where $H_{solid}$ is the concentration of hydrogen in the metal, $K_S$ is Sievert's constant and $P$ is the equilibrium hydrogen pressure. When the terminal solubility of hydrogen in the α phase is exceeded the hydride phase precipitates and is designated the β phase. Upon the appearance of the β phase the equilibrium pressure will remain constant and the isotherm forms a plateau as more hydrogen is added. When the phase conversion is complete the system regains a degree of freedom and the pressure again rises as a function of the hydrogen content. In many systems there is a significant hysteresis effect in the phase conversion process which is reflected by a higher isotherm plateau pressure for the α⇒β conversion than the reverse α⇐β process.

The reaction of a metal with hydrogen gas may be written as

$$M + \frac{x}{2}H_2 \Leftrightarrow MH_x \quad (2)$$

*Corresponding author.

0925-8388/99/$ – see front matter 
PII: S0925-8388(99)00413-2

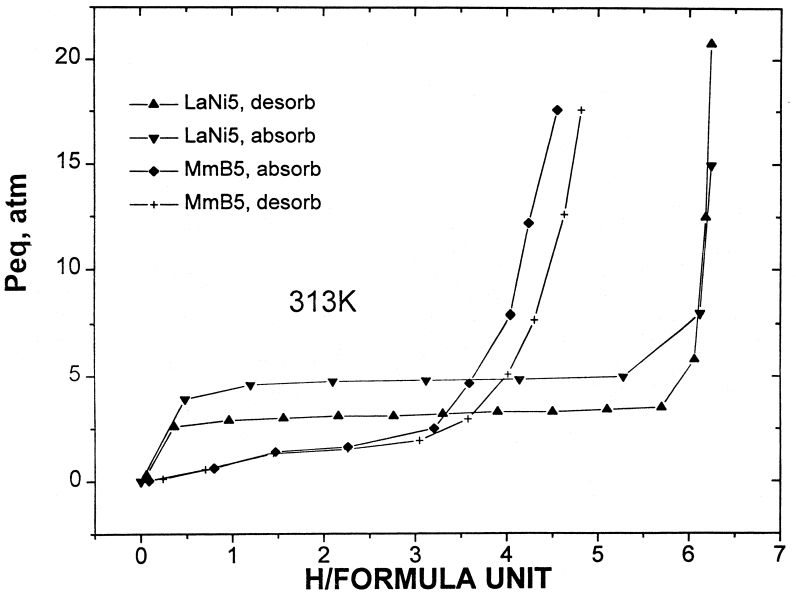


Fig. 1. PC isotherms for $LaNi_5$ and $MmNi_{3.55}Co_{0.75}Mn_{0.4}Al_{0.3}$ (Ref. [43]).

Thermodynamic quantities for a system may be determined from the van't Hoff equation,

$$\ln P_{H_2} = \frac{2}{x}(\Delta H/RT) + C \quad (3)$$

The enthalpy of the phase conversion can be determined via Eq. (3) by plotting the log of the absorption or desorption plateau pressure, $P_{plateau}$ vs. the reciprocal temperature as indicated in Fig. 4. When the solubility of hydrogen in the metal (α) phase is small then $\Delta H$ is essentially the enthalpy of formation of the hydride from the metal [5]; the intercept, $C$, is equal to $(-2/x)(\Delta S/R)$. Eq. (3) is commonly presented as (4)

$$\ln P_{plateau} = \frac{A}{T} + B \quad (4)$$

where the constants $A$ and $B$ are specified. Thermodynamic data for some representative alloys are given by Sandrock [1].

## 3. Reaction rules and predictive theories

There have been numerous studies with the object of gaining an understanding of the factors that influence the stability, stoichiometry and H site occupation in hydride phases. Stability has been correlated with cell volume [6] or the size of the interstitial hole in the metal lattice [7] and the free energy of the α⇔β phase conversion. This has been widely exploited to modulate hydride phase stability as discussed in Section 6.1 and is particularly important in electrochemical applications.

Westlake developed a geometric model which is fairly successful in predicting site occupation in $AB_5$ and $AB_2$ hydride phases [8]. It involves two structural constraints; that the minimum hole size necessary to accommodate a H atom has a radius of 0.40 Å and that the minimum distance between two H occupied sites is 2.10 Å. The former criterion was empirically derived from a survey of known hydride structures while the latter was suggested by Switendick based on electronic [9] band structure calculations.

A relatively simple set of rules have been found to hold for all intermetallic hydrides useful for hydrogen storage [10]. They may be stated as follows.

1. In order for an intermetallic compound to react directly and reversibly with hydrogen to form a hydride phase it is necessary that at least one of the metal components be capable of forming a stable binary hydride.
2. If a reaction takes place at a temperature at which the metal atoms are mobile, the system will assume its most favored thermodynamic configuration.
3. If the metal atoms are not mobile (low temperature reactions) intermetallic hydride phases can only have crystal structures that are very similar to the starting intermetallic compound. In effect the system may be considered to be pseudo-binary as the metal atoms behave as a single component.

## 4. Metal hydride–nickel batteries

The half cell reactions taking place in a $MH_x$/Ni battery may be written as follows:

$$MH_x + xOH^- \Leftrightarrow M + xH_2O + xe^- \quad (5)$$

$$Ni(OOH) + H_2O + e^- \Leftrightarrow Ni(OH)_2 + OH^- \quad (6)$$

It is in effect a rocking chair type battery in which hydrogen is transferred from one electrode to the other. It is most convenient that the voltage is essentially the same as the conventional nicad batteries.

Two types of metal hydride electrodes, namely the $AB_5$ and $AB_2$ classes of intermetallic compounds, are currently of interest. The $AB_5$ electrode alloys have the hexagonal $CaCu_5$ structure where the A component comprises one or more rare earth elements and B consists of Ni plus minor amounts of other metals. The paradigm compound of this class is $LaNi_5$ which has been well investigated because of its utility in conventional hydrogen storage applications. Unfortunately $LaNi_5$ is too unstable and too corrosion sensitive for use as a battery electrode. Thus commercial $AB_5$ electrodes use mischmetal, a low cost combination of rare earth elements, as a substitute for La. The $B_5$ component remains primarily Ni but is substituted in part with Co, Mn, Al etc. The partial substitution of Ni increases thermodynamic stability of the hydride phase [11] and corrosion resistance. Such an alloy is commonly written as $MmB_5$ where Mm represents the mischmetal component. The nominal compositions of commercially obtained normal and cerium-free mischmetal are given in Table 1.

The other electrode type, not yet widely used in batteries, is usually referred to as the $AB_2$ or Laves phase type electrodes and is discussed in Section 11. These electrodes are complicated, multiphase alloys with as many as nine metal components. Alloy formulation is primarily an empirical process where the composition is adjusted to provide one or more hydride forming phases in the particle bulk and has a surface that is presumed to be corrosion resistant because of the formation of semi-passivating oxide layers. Unlike the $AB_5$ alloys there are few systematic guidelines which can be used to predict alloy properties. Eventually $AB_2$ alloy electrodes may be more attractive than $AB_5$ electrodes in terms of cost and energy density but currently that potential is far from realized.

There are also other intermetallic hydrides that have largely been ignored for battery applications because they are too stable, electrochemically inactive or, most importantly, subject to severe corrosion in the battery environment. Alloys such as $Mg_2Ni$ [12] and FeTi [13], have substantially greater hydrogen storage capacity than the conventional $AB_5$ and $AB_2$ alloys and are less costly; unfortunately neither has been demonstrated to have attractive electrochemical properties. High content Mg amorphous alloys, produced by mechanical alloying, have exhibited initial storage capacities of $>400$ mAh/g but they rapidly deteriorate upon cycling [14]. A novel vanadium based electrode, $TiV_3Ni_{0.56}$ has also been shown to have a high initial storage capacity, 400–450 mAh/g, but also corrodes rapidly upon electrochemical cycling [15]. Super-stoichiometric $La(Ni, Sn)_{5+x}$ alloys are also of interest and will be discussed in Section 10.

Table 1
Composition of mischmetal[a]

| Rare earth | Normal[b], wt.% | Ce free[c], wt.% |
|---|---|---|
| Ce | 56.9 | 0.13 |
| La | 20.5 | 58.2 |
| Nd | 14.7 | 29.9 |
| Pr | 5.5 | 7.6 |
| Fe | 0.42 | 0.07 |
| O | 0.058 | 0.47 |
| C | 0.032 | 0.104 |
| N | 0.002 | 0.162 |
| Y | $<0.01$ | 0.04 |
| Ca | 0.13 | 0.27 |

[a] Analyzed at Materials Preparation Center, Ames Lab., Ames, IA.
[b] From Molycorp, Washington, PA, USA.
[c] From Ergenics, Wyckoff, NJ, USA.

## 5. Alloy activation

Essentially all metals and alloys which form metallic hydrides require an activation process before the metal will readily cycle between the hydride and metal phase. All the $AB_5$ and $AB_2$ alloys are quite brittle and during the activation procedure are pulverized to fine particles. This greatly enhances subsequent reaction rates. The surface composition of $LaNi_5$ after activation has been defined by X-ray photoemission spectroscopy, Auger electron spectroscopy and magnetic susceptibility studies [16]. There is a surface enrichment of La to give a ratio of $La/Ni \approx 1$; the La is associated with oxygen but Ni remains metallic and is present as clusters on the surface containing about 6000 atoms. This is the mechanism by which catalytic metal surface sites are formed for chemical or electrochemical reactions. The activation procedure is straightforward; in gas/solid systems it merely consists of repeated formation and decomposition of the hydride phase [17]. Electrochemical activation also consists of repeated charge and discharge cycles which sometimes requires extended cycling periods.

## 6. $AB_5$ electrodes

The use of $LaNi_5$ as an electrode was reported by Justi in 1973 [18]. However the capacity was less than 1/3 that of 372 mAh/g which corresponds to the discharge of six hydrogens from $LaNi_5H_6$, probably due to its dissociation pressure of $>1$ atm at 298 K. Thus, in an open cell most of the hydrogen is lost as $H_2$ gas. A few years later Percheron-Guegan [19] and van Rikswick [20] substituted other metals in part for nickel thereby increasing hydride stability and charge capacity. However, this did not solve the electrode corrosion problem also observed with $LaNi_5$. In 1984 Willems [21] prepared the first multicomponent $AB_5$ electrode that had an acceptable cycle life. He reported the positive correlation between lattice expansion

and electrode corrosion. Finally in 1987 an alloy of composition $MmNi_{3.55}Co_{0.75}Mn_{0.4}Al_{0.3}$ was shown to meet the minimum requirements for a practical battery with respect to cost, cycle life and storage capacity [22,23]. Indeed this composition is very similar to those currently used in commercial Ni–MH batteries with $AB_5$ hydride anodes. Ikoma et al. [24] describe an experimental EV (electric vehicle) battery having an energy density of 70 Wh/kg using an anode of composition Mm(Ni, Co, Mn, $Al)_5$. The electrochemical behavior of this alloy and its relation to small changes in alloy composition is of great practical interest and will be discussed at length herein.

### *6.1. Pertinent properties of $AB_5$ electrode alloys*

In order to fully understand the electrochemical behavior of $AB_5$ hydrides a knowledge of their chemical and structural properties is required. Van Vucht et al. [25] were the first to prepare $LaNi_5$ hydride and it is arguably the most thoroughly investigated H storage compound. It reacts rapidly with hydrogen at room temperature at a pressure of several atmospheres above the equilibrium plateau pressure. PC isotherms for this system are shown in Fig. 1. The nominal reaction may be written as

$$LaNi_5 + 3H_2 \Leftrightarrow LaNi_5H_6 \quad (7)$$

With reference to rule 3 (Section 3) regarding metal atom mobility, we note that $\Delta G_f$ at 298 K for $LaNi_5$ and for $LaH_2$ are about $-67$ and $-171$ kJ, respectively. Thus the following disproportionation reaction is highly favored [26],

$$LaNi_5 + H_2 \Rightarrow LaH_2 + 5Ni \quad \Delta G_{298\,K} = -104\,kJ \quad (8)$$

whereas for reaction (7) $\Delta G_{298} \approx 0$, but at low temperatures it does not take place under normal conditions. However, thermodynamics is not to be denied indefinitely and after many ($>1000$) hydriding dehydriding cycles some disproportionation does take place as evidenced by isotherm distortion and reduction in H storage capacity [27].

The kinetics of the formation and decomposition of $LaNi_5$ hydride have been widely studied with widely varying results [28] due to the difficulty in maintaining isothermal conditions. When kinetic experiments were carried out isothermally or nearly so, the kinetics were well described by a shrinking core model [29,30]. In this model the rate limiting process is the solid state transformation taking place at the interface between the $\alpha$ and $\beta$ phases.

A particular advantage of the $AB_5$ hydride family is that the properties of the alloy–hydrogen system can be widely varied by substituting, in whole or in part, other metals for La and Ni. For example, normal mischmetal when substituted for La in $LaNi_5$ forms a hydride having about the same hydrogen content but is much more unstable [31]. Lundin et al. [7] carried out a systematic study of such substitutional alloys and correlated the free energy of formation (plateau region) with the change of the interstitial hole size caused by the substituted metal component. Gruen et al. [6] have taken a similar approach, but rather correlate the cell volume with $\ln P_{plateau}$, as shown in Fig. 3. This correlation has been widely exploited to prepare $AB_5$ alloys that form hydride phases having a stability within the range desirable for battery applications.

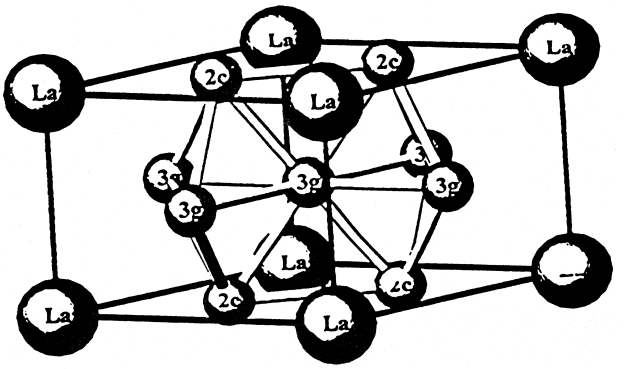


Fig. 2. Metal lattice of $LaNi_{3.55}Co_{0.75}Mn_{0.4}Al_{0.3}$. Co is located on both the basal and the midplane. Mn and Al are located only on the midplane. See Table 4 (Ref. [33]).

### *6.2. Crystal structure of $LaNi_{3.55}Co_{0.75}Mn_{0.33}Al_{0.30}$*

The crystal structure of this complex $AB_5$ alloy and its deuteride have been determined by Latrouche et al. [32] and by Vogt et al. [33] using neutron diffraction. Both the metal and the deuteride phase are in space group P6/mmm. The latter investigators adjusted the isotopic ratio of Ni in the sample to give a zero scattering length for neutron diffraction; this increased the scattering contribution of cobalt from 3.8 to 15.2% thereby improving the reliability of the determination of the cobalt site location. The structural data given by Vogt et al. [33] places 31% of the Co on the 2c site and 69% on the 3g site (see Fig. 2).

It is of interest to note that the structure of $LaNi_5D_7$ is quite different from the above complex deuteride [34,35]. The space group of $LaNi_5D_7$ is $P6_3mc$ and is due to the formation of a superlattice that requires a doubling of the unit cell along the *c* axis. This is a consequence of deuterium occupying alternate Ni tetrahedra along the *c* direction due to the constraint on the minimum D–D distance of 2.10 Å. No such superlattice occurs in the complex $AB_5$ alloy because of the disorder caused by substitution of Co, Al and Mn for Ni.

## 7. Preparation of $AB_5$ electrodes

Electrode behavior is strongly influenced by alloy microstructure, metal stoichiometry and composition [36]. Percheron-Guegan and Welter have described both laboratory and industrial preparation techniques for many inter-

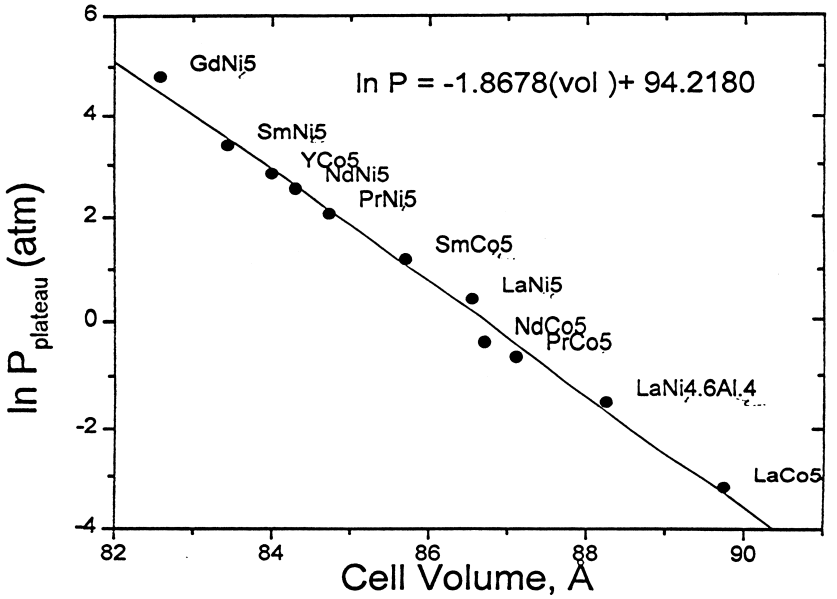


Fig. 3. Alloy cell volume vs. ln $P_{plateau}$ for various $AB_5$ type hydrides (Ref. [6]).

metallic hydride formers, particularly emphasizing $LaNi_5$ and its substituted analogues [37].

Since all $AB_5$ alloys are pulverized to fine particles in the activation process, electrodes must be designed to accommodate fine powders as the active material. There are several methods of electrode fabrication [36]. The fabrication of a simple paste electrode suitable for laboratory studies is reported by Petrov et al. [38].

## 8. Hydride electrodes and temperature

Hydride phase stability is a logarithmic function of the temperature and must be taken into account when choosing an electrode composition. For example, the equilibrium plateau pressure (decomposition) of $LaNi_5H_x$ at 65°C≈10 atm; much too high for use as a battery electrode. Van't Hoff plots [39] for $LaNi_5H_x$, $MmNi_{3.55}Co_{0.75}Mn_{0.4}Al_{0.3}H_x$ and $Mm^*Ni_{3.55}Co_{0.75}Mn_{0.4}Al_{0.3}H_x$ (Mm* = cerium-free mischmetal, Table 1) are shown in Fig. 4. At 65°C the absorption plateau pressure of $Mm^*B_5$ would be 0.5 atm whereas that of $MmB_5$ is 5.0 atm. Thus, even though both mischmetal electrodes have similar electrochemical properties at room temperature, only the former would be suitable for battery use at higher temperatures. The high Ce content of normal mischmetal is responsible for the hydride phase instability.

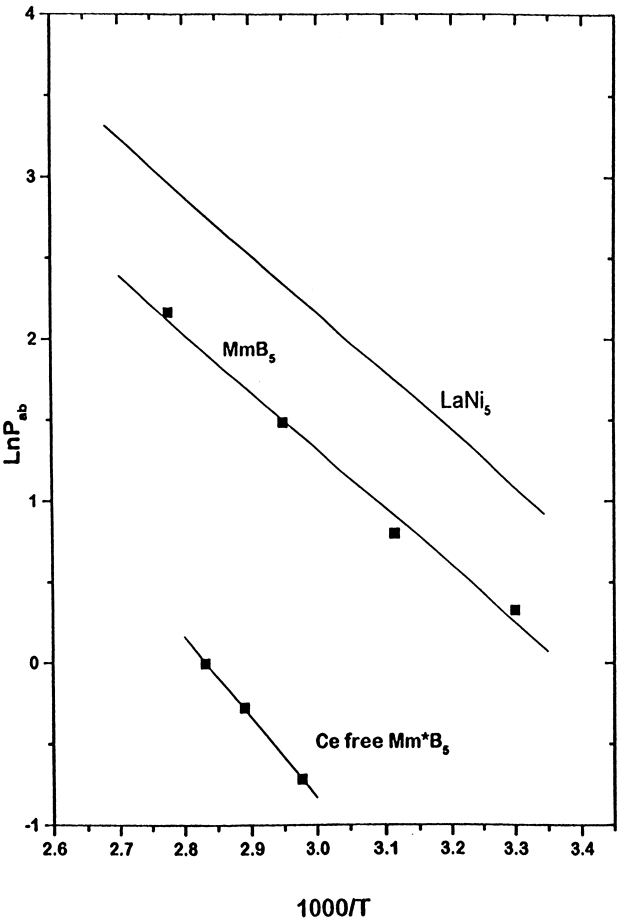


Fig. 4. Van't Hoff plots for $LaNi_5H_x$, $MmNi_{3.55}Co_{0.75}Mn_{0.4}Al_{0.3}H_x$ and $Mm^*Ni_{3.55}Co_{0.75}Mn_{0.4}Al_{0.3}H_x$ (Ref. [39]).

## 9. Electrode corrosion and storage capacity

Deterioration of electrode performance due to corrosion of electrode components is a critical problem. The suscep-

tibility of $MH_x$ electrodes to corrosion is essentially determined by two factors; surface passivation due to the presence of surface oxides or hydroxides and the molar volume of hydrogen, $V_H$, in the hydride phase. As pointed out by Willems and Buschow [40], $V_H$ is important since it governs alloy expansion and contraction during the charge–discharge cycle. Large volume changes increase the flushing action of the electrolyte through the pores and microcracks of the electrode during each charge and discharge cycle thereby increasing the rate of contact of the alloy surface with fresh electrolyte and, consequently, the corrosion rate. Thus, when examining the effect of various substituents upon electrode corrosion the question arises whether an observed change is due to a change in lattice expansion or to a change in surface passivation, e.g. the formation of a corrosion resistant oxide layer. $V_H$ is given for a number of alloys in Tables 2 and 3.

While the partial substitution of Ni by other metals has ameliorated the corrosion problem it has also resulted in a reduced storage capacity and high alloy costs primarily because of the incorporation of Co. Almost all multi-component hydrides have less storage capacity than $LaNi_5H_x$ due to the partial substitution of Ni. Percheron-Guegan et al. [41] noted this with the ternary alloy $LaNi_{5-x}M_x$, with M = Al, Mn, Si or Cu. Thus, although the cycle life of substituted $AB_5$ electrodes is greatly extended over that of $LaNi_5$ a severe penalty in storage capacity is exacted for this improvement as illustrated by the PCT diagram in Fig. 1. It is also of interest to note that $LaNi_5$ exhibits a significant hysteresis effect while $MmNi_{3.55}Co_{0.75}Mn_{0.4}Al_{0.3}$ does not. A small hysteresis effect in complex $AB_5$ hydrides is not unusual, but it is almost always appreciable in simpler systems [1].

### 9.1. Corrosion and composition

The long life of $MmB_5$ battery electrodes raises the question: why do such electrodes behave so differently compared to other more simple formulations? Such differences are very apparent in plots of charge capacity vs. charge–discharge cycles as reported by Adzic et al. [42] and shown in Fig. 5. Four different electrodes are compared Mm(or Mm*)$Ni_{3.55}Co_{0.75}Mn_{0.4}Al_{0.3}$ (Mm* refers to Ce-free mischmetal) and two similar, but Co-free, electrodes. The latter electrodes rapidly corrode. Obviously alloy composition is responsible for the observed behavior and is discussed in the following sections. The results of these experiments are summarized in Table 3. While cycle life may differ dramatically, inspection of cycle life plots reveals a common behavior which is found in almost all $MH_x$ electrodes. There is an initial steep increase in capacity which comprises the activation process. After activation a maximum in electrochemical storage capacity, $Q_{max}$, is reached. This is usually followed by an almost

Table 2
Crystallographic parameters and $V_H$ of selected alloys

| Composition | $a$ (Å) | $c$ (Å) | Cell vol. (Å$^3$) | $V_H$ (Å$^3$) | Ref. |
|---|---|---|---|---|---|
| $NdNi_{3.55}Co_{0.75}Mn_{0.4}Al_{0.3}$ | 4.9992 | 4.0221 | 87.05 | 2.66 | [b] |
| $La_{0.25}Nd_{0.75}Ni_{3.55}Co_{0.75}Mn_{0.4}Al_{0.3}$ | 5.0138 | 4.0254 | 87.63 | 2.74 | [b] |
| $LaNi_{3.55}Co_{0.75}Mn_{0.4}Al_{0.3}$ | 5.0642 | 4.0325 | 89.56 | 2.93 | 42 |
| $La_{0.65}Pr_{0.35}Ni_{3.55}Co_{0.75}Mn_{0.4}Al_{0.3}$ | 5.0368 | 4.0206 | 88.33 | 2.97 | [b] |
| $LaNi_{3.5}Co_{0.75}Mn_{0.4}Al_{0.3}$ | 5.0699 | 4.0392 | 89.91 | 3.00 | 42 |
| $Mm_{0.3}Mm^*_{0.7}Ni_{3.55}Co_{0.75}Mn_{0.4}Al_{0.3}$ | 5.0234 | 4.0434 | 88.36 | 3.00 | [b] |
| $LaNi_{3.95}Co_{0.75}Al_{0.3}$ | 5.0378 | 4.0107 | 88.15 | 3.02 | 50 |
| $MmNi_{3.55}Co_{0.75}Mn_{0.4}Al_3$ Ce free | 5.0318 | 4.0309 | 88.38 | 3.05 | 50 |
| $LaNi_{3.55}Co_{0.75}Mn_{0.4}Al_{0.3}$ | 5.0615 | 4.0298 | 89.40 | 3.06 | 42 |
| $La_{0.5}Nd_{0.5}Ni_{3.55}Co._{0.75}Mn_{0.4}Al_{0.3}$ | 5.0315 | 4.0259 | 88.26 | 3.07 | [b] |
| $LaNi_{3.55}Co_{0.75}Mn_{0.3}Al_{0.3}$ | 5.0662 | 4.0321 | 89.70 | 3.07 | 50 |
| $LaNi_{4.1}Co_{0.2}Mn_{0.4}Al_{0.3}$ | 5.0609 | 4.0361 | 89.52 | 3.09 | 41 |
| $LaNi_{3.9}Co_{0.4}Mn_{0.4}Al_{0.3}$ | 5.0629 | 4.0349 | 89.57 | 3.09 | 41 |
| $MmNi_{3.55}Co_{0.75}Mn_{0.4}Al_{0.3}$ [a] | 4.9890 | 4.0545 | 87.39 | 3.10 | 42 |
| $MmNi_{3.55}Co_{0.75}Mn_{0.4}Al_{0.3}$ | 4.9626 | 4.0560 | 86.50 | 3.13 | 42 |
| $La_{0.25}Ce_{0.75}Ni_{3.55}Co_{0.75}Mn_{0.4}Al_{0.3}$ | 4.9538 | 4.0559 | 86.19 | 3.15 | 42 |
| $La_{0.5}Ce_{0.5}Ni_{3.55}Co_{0.75}Mn_{0.4}Al_{0.3}$ | 4.9934 | 4.0446 | 87.33 | 3.15 | 42 |
| $La_{0.65}Nd_{0.35}Ni_{3.55}Co_{0.75}Mn_{0.4}Al_{0.3}$ | 5.0324 | 4.0211 | 88.19 | 3.15 | [b] |
| $LaNi_{3.55}Co_{0.75}Mn_{0.14}Al_{0.3}$ | 5.0509 | 4.0321 | 89.08 | 3.16 | 50 |
| $LaNi_{3.85}Co_{0.75}Mn_{0.38}$ | 5.0526 | 4.0195 | 88.86 | 3.20 | 50 |
| $La_{0.8}Ce_{0.2}Ni_{3.55}Co_{0.75}Mn_{0.4}Al_{0.3}$ | 5.0380 | 4.0416 | 88.84 | 3.21 | 42 |
| $MmNi_{3.5}Co_{0.75}Mn_{0.4}Al_{0.3}$ | 4.9623 | 4.0456 | 86.27 | 3.23 | 42 |
| $LaNi_{4.3}Mn_{0.4}Al_{0.3}$ | 5.0591 | 4.0370 | 89.48 | 3.26 | 41 |
| $La_{0.65}Ce_{0.35}Ni_{3.55}Co_{0.75}Mn_{0.4}Al_{0.3}$ | 5.0168 | 4.0451 | 88.16 | 3.24 | 42 |
| $LaNi_{3.85}Co_{0.75}Mn_{0.4}$ | 5.0494 | 4.0034 | 88.39 | 3.35 | 50 |
| $LaNi_{4.7}Al_{0.3}$ | 5.0195 | 4.0076 | 87.44 | 3.47 | 42 |
| $MmNi_{4.3}Mn_{0.4}Al_{0.3}$ | 4.9652 | 4.0453 | 86.37 | 3.51 | 41 |

[a] Synthetic mischmetal i.e. $La_{0.26}Ce_{0.52}Pr_{0.06}Nd_{0.16}$.
[b] J.R. Johnson, unpublished data.

Table 3
Effect of B substitution in $La(NiCoMnAl)_5$ electrodes (Ref. [51])

| $x$ value | $V_H$ (Å$^3$) | $Q_{max}$ mAh/g | $n$, H atoms per unit cell | $\Delta V/V$% | Corrosion wt.%/cycle |
|---|---|---|---|---|---|
| Effect of Co in $LaNi_{4.3-x}Co_xMn_{0.4}Al_{0.3}$ | | | | | |
| 0.75 | 2.99 | 330 | 5.18 | 17.3 | 0.139 |
| 0.40 | 3.09 | 334 | 5.25 | 18.1 | 0.257 |
| 0.20 | 3.09 | 334 | 5.25 | 18.1 | 0.380 |
| 0.0 | 3.26 | 324 | 5.09 | 18.5 | 0.485 |
| Effect of Al in $LaNi_{3.85-x}Co_{0.75}Mn_{0.4}Al_x$ | | | | | |
| 0.2 | 3.01 | 314 | 4.98 | 16.66 | 0.127 |
| 0.3 | 2.99 | 330 | 5.18 | 17.33 | 0.139 |
| 0.1 | 3.01 | 327 | 5.22 | 17.58 | 0.290 |
| 0.0 | 3.20 | 353 | 5.66 | 20.39 | 0.407 |
| 0.0 | 3.35 | 366 | 5.88 | 22.30 | 0.412 |
| Effect of Mn in $LaNi_{3.95-x}Co_{0.75}Mn_xAl_{0.3}$ | | | | | |
| 0.14 | 3.16 | 320 | 4.87 | 17.27 | 0.106 |
| 0.40 | 2.99 | 330 | 5.18 | 17.33 | 0.139 |
| 0.0 | 3.02 | 340 | 5.37 | 18.38 | 0.167 |
| 0.30 | 3.07 | 353 | 5.48 | 18.75 | 0.150 |
| Effect of Co in $MmNi_{4.3-x}Co_xMn_{0.4}Al_{0.3}$ electrodes | | | | | |
| 0.75 | 3.13 | 247 | 3.90 | 14.3 | 0.001 |
| 0.75[a] | 3.05 | 295 | 4.64 | 16.0 | 0.041 |
| 0 | 3.5 l | 314 | 4.96 | 20.1 | 0.354 |
| 0[a] | 3.14 | 314 | 4.94 | 17.7 | 1.029 |

[a] Cerium-free Mm.

linear decrease in capacity which may be termed capacity decay, defined as the slope of the capacity vs. cycle curve, i.e. $-dQ/dcycle$.

In order to elucidate the relationship between corrosion rate and composition Adzic et al. [43] used the following approach. The H content of the charged electrode, expressed as the number of H atoms, $n$, per formula unit, was calculated from $Q_{max}$ via the Faraday equation,

$$n = e^- = \frac{3600}{9.65 \times 10^7}(M_w)(Q_{max}) \quad (9)$$

where $M_w$ is the molecular weight of the alloy and $Q$ is in units of mAh/g. The percent lattice expansion of the unit cell in each electrochemical cycle was calculated via

$$\%\frac{\Delta V}{V} = \left(\frac{V_H}{V}\right) \times n \times 100 \quad (10)$$

where $\Delta V$ is the actual volume change of the unit cell in Å$^3$ in each charge or discharge cycle, $V$ is the initial unit cell volume and $n$ is the number of H atoms inserted into the unit cell and subsequently discharged. Further, the loss of electrochemical capacity is directly proportional to the loss of the $AB_5$ alloy by oxidation and readily calculated as follows:

$$\frac{\%\text{wt. loss}}{\text{cycle}} = \frac{-dQ}{dcycle}(Q_{max})^{-1} \times 100 \quad (11)$$

They [43] employed the above equations to determine the effects of Ce, Co, Al and Mn upon the electrochemical performance of $La(NiCoMnAl)_5$ electrodes as discussed below.

### 9.2. Effect of cerium

The rare earth composition of commercial electrodes is also related to electrode corrosion. Sakai et al. [44] noted that the presence of Nd and Ce inhibited corrosion when substituted in part for La in $La_{1-x}Z_x(NiCoAl)_5$ (Z=Ce or

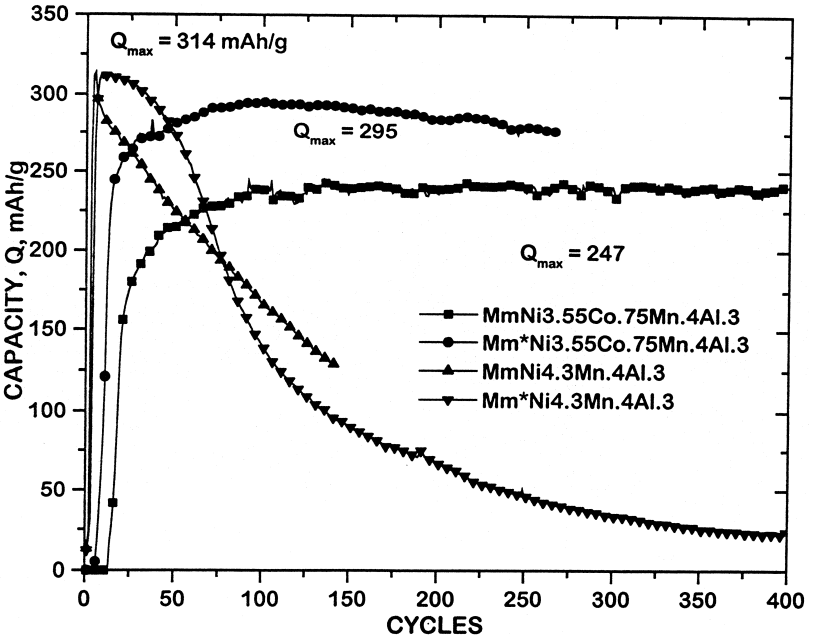


Fig. 5. Charge capacity, $Q$, vs. charge–discharge cycles for four mischmetal $AB_5$ electrodes. Note high decay rate in charge capacity for Co-free electrodes (Ref. [42]).

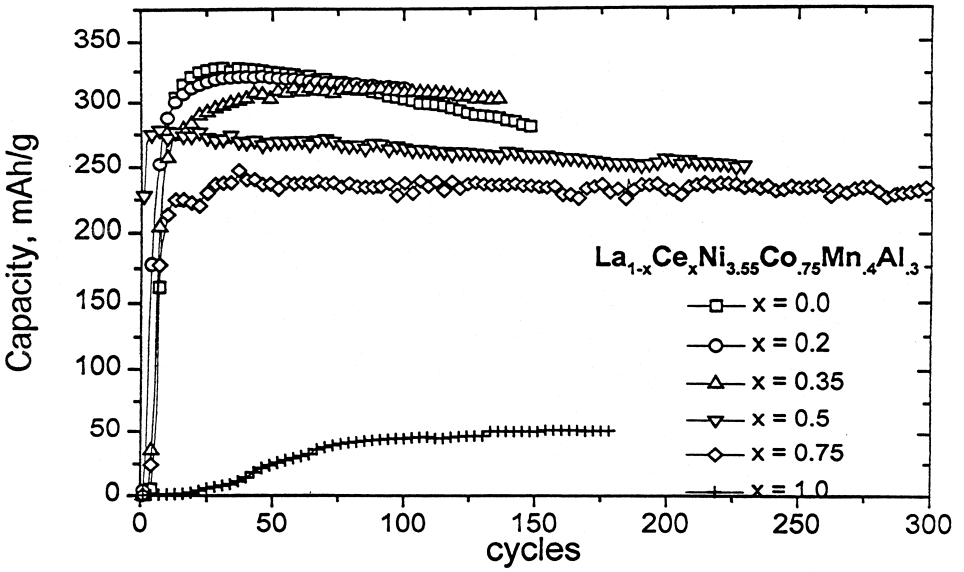


Fig. 6. Charge capacity, $Q$, vs. charge–discharge cycles for $La_{1-x}Ce_xNi_{3.55}Co_{0.75}Mn_{0.4}Al_{0.3}$ electrodes (Ref. [42]).

Nd) electrodes. Willems [21] prepared an electrode having the composition of $La_{0.8}Nd_{0.2}Ni_{2.5}Co_{2.4}Si_{0.1}$ which retained 88% of its storage capacity after 400 cycles. He attributed its long cycle life to a low $V_H$ of 2.6 Å$^3$.

The case of cerium is of particular interest. Adzic et al. [43] examined the electrochemical properties of a homologous series of alloys with a composition corresponding to $La_{1-x}Ce_xNi_{3.35}Co_{0.75}Mn_{0.4}Al_{0.3}$. They also present a PCT diagram which shows that at $x>0.2$ there is a decrease in the H storage capacity and thermodynamic stability until at $x=1$ the decreases in both parameters are marked. This conforms with the decrease in the unit cell volume with Ce content.

Cycle life plots for the $La_{1-x}Ce_xB_5$ electrodes are illustrated in Fig. 6. The decreased charge capacity found in all $La_{1-x}Ce_xB_5$ alloys with $x>0.35$ conforms to the shorter lengths and higher plateau pressures of the isotherms as noted by Adzic et al. [42]. The low electrochemical capacity of $CeB_5$ is a consequence of the high dissociation pressure of the hydride phase.

The corrosion rates for the $La_{1-x}Ce_xB_5$ electrodes are listed in Table 4. The data clearly show a reverse correlation between lattice expansion and corrosion; thus one concludes that the corrosion inhibition stemming from the presence of Ce is due to a surface effect. This conclusion is supported by previous work reporting that a film of $CeO_2$

Table 4
Effect of Ce in $La_{1-x}Ce_xNi_{3.55}Co_{0.75}Mn_{0.4}Al_{0.3}$ electrodes (Ref. [43])

| $x$ value | $V_H$ Å$^3$/atom | $n$, H atoms per unit cell | %$\Delta V/V$ | $Q_{max}$ mAh/g | Corrosion wt.%/cycle |
|---|---|---|---|---|---|
| 1.0 | 1.6[a] | 0.8 | 1.4625 | 51 | 0 |
| 0.75 | 3.15 | 3.8 | 13.919 | 241 | 0.003 |
| 0.5 | 3.15 | 4.4 | 15.917 | 278 | 0.04 |
| 0.20 | 3.21 | 4.8 | 17.534 | 305 | 0.042 |
| 0.20 | 3.21 | 4.6 | 16.547 | 293 | 0.047 |
| 0.50 | 3.15 | 4.0 | 14.634 | 260 | 0.054 |
| 0.20 | 3.21 | 4.6 | 16.659 | 293 | 0.051 |
| 0.20 | 3.21 | 5.0 | 18.122 | 318 | 0.057 |
| 0.35 | 3.24 | 5.0 | 18.376 | 318 | 0.057 |
| 0.20 | 3.21 | 5.0 | 18.112 | 318 | 0.066 |
| 0.0 | 2.99[b] | 4.8 | 15.96 | 305 | 0.15 |
| 0.0 | 2.99[b] | 5.2 | 17.33 | 331 | 0.139 |
| 0.0 | 2.99[b] | 5.1 | 17.002 | 325 | 0.145 |
| $LaNi_{4.7}Al_{0.3}$[c] | 3.47 | 4.5 | 17.943 | 285 | 0.291 |

[b] Average.
[c] Included for comparison.
[a] α phase.

on metal surfaces inhibits corrosion [45]. XAS (X-ray absorption spectroscopy) studies (Section 12) confirm the corrosion inhibition effect of Ce [46].

### 9.3. Effect of cobalt

Cobalt is invariably present in commercial $MH_x$ battery electrodes. However, it is also expensive and substantially increases battery costs. Willems and Buschow [40] attributed reduced corrosion in $LaNi_{5-x}Co_x$ ($x=1$ to 5) to low $V_H$. Sakai et al. [47] noted that $LaNi_{2.5}Co_{2.5}$ was the most durable of a number of substituted $LaNi_{5-x}Co_x$ alloys but it also had the lowest storage capacity.

The results of a systematic study [42] of the effect of Co in an alloy series corresponding to $LaNi_{4.3-x}Co_xMn_{0.4}Al_{0.3}$ is shown in Fig. 7 and summarized in Table 3. The correlation between expansion and corrosion is rather weak; e.g. even though the H content is constant at $x=0.2$ and 0.4, corrosion is increased while expansion is unchanged. It is thus likely that corrosion inhibition by Co is also due to a surface effect as with Ce. Kanda et al. [48] found evidence that Co suppresses the transport of Mn to the surface where it is readily oxidized causing rapid electrode deterioration. Recent XAS results also suggest that Co inhibits corrosion via a surface process by suppressing Ni oxidation [49].

### 9.4. Effect of aluminum

Aluminum appears to be present in all commercial $AB_5$ electrodes. Sakai et al. [50] noted that the incorporation of Al in $La(NiCoAl)_5$ alloys substantially reduced electrode corrosion and attributed this to the formation of protective surface oxides. The corrosion inhibiting effect of Al is clearly shown in Fig. 8 which plots storage capacity versus cycle life for $LaNi_{3.85-x}Co_{0.75}Mn_{0.4}Al_x$ electrodes [51]. As illustrated in Table 3 the presence of even a small amount of Al substantially decreases $V_H$, $n$ and, consequently, both lattice expansion and corrosion.

### 9.5. Effect of manganese

Manganese is also present in most commercial electrodes. In a series of experiments examining the cycle lives of a homologous alloy series, $LaNi_{5-x}M_x$ (M=Mn, Cu, Cr, Al and Co), Sakai et al. [50] noted that Mn was the least effective in improving performance. In the more complex alloy examined by Adzic et al. [51] the function of Mn is still open to question. The cyclic behavior of a set of electrodes of varying Mn content is shown in Fig. 9. It apparently increases $V_H$ (Table 3) slightly and although the correlation between lattice expansion, $n$, and corrosion rate is fairly strong it is not a function of Mn content.

## 10. Non-stoichiometric $AB_{5+x}$ alloys

Notten et al. [52,53] reported that the electrochemical cycling stability can be improved dramatically when using non-stoichiometric $La(NiCu)_{5+x}$ alloys. They attributed such improvement to an alteration of the crystal structure in which the excess of B-type atoms is accommodated in the $AB_5$ lattice by the occupation of empty A sites (La) with dumbbell pairs of Ni atoms oriented along the $c$-axis while preserving the P6/mmm space group. A representation of the $AB_{5+x}$ lattice is shown in Fig. 10. Recently Vogt et al. have shown that the structure of $La_{0.9}Ni_{4.54}Sn_{0.32}$ (a stoichiometry of $AB_{5.40}$ when La is

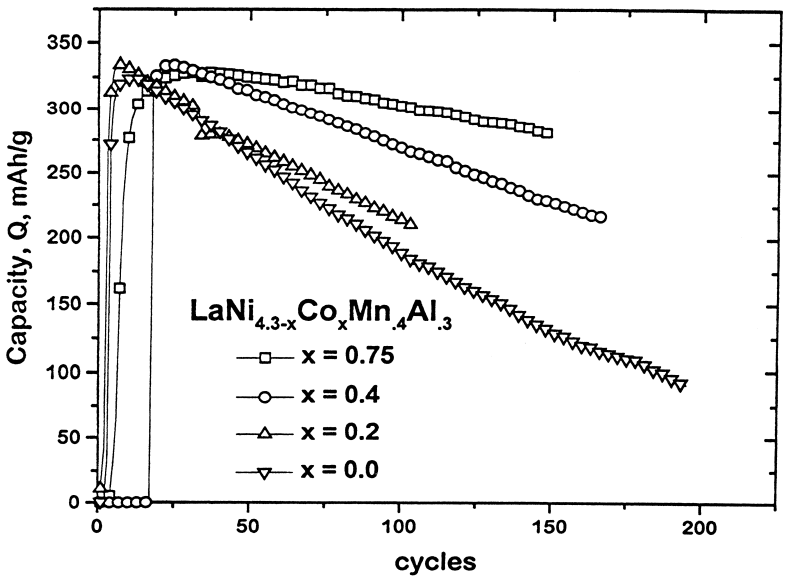


Fig. 7. Charge capacity, $Q$, vs. charge–discharge cycles for $LaNi_{4.3-x}Co_xMn_{0.4}Al_{0.3}$ electrodes (Ref. [42]).

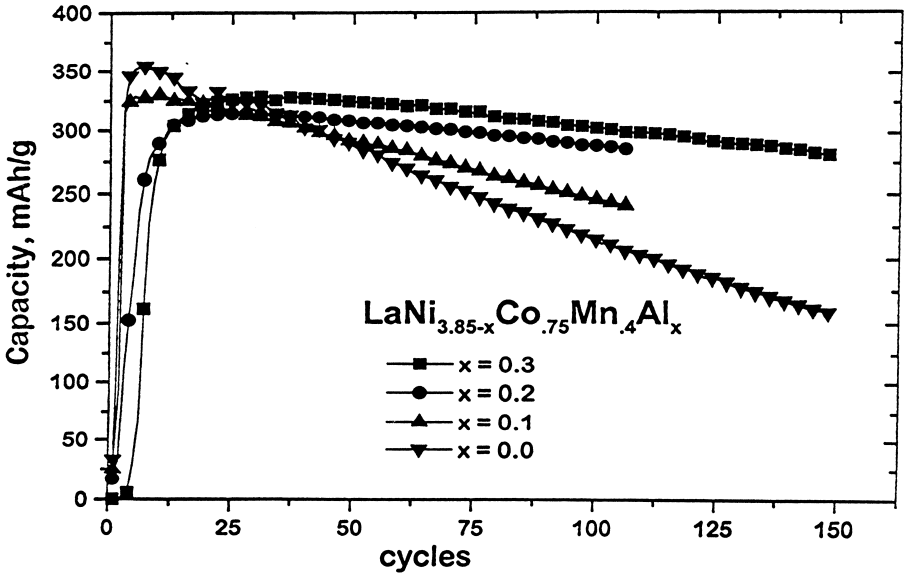


Fig. 8. Charge capacity, $Q$, vs. charge–discharge cycles for $LaNi_{3.85-x}Co_{0.75}Mn_{0.4}Al_x$ electrodes (Ref. [51]).

normalized) compensates for La deficiency by also inserting Ni dumbbells in empty A sites [54], whereas Sn occupies the midplane 3g site exclusively. Here too the presence of Ni dumbbells greatly improves electrode cycle life compared to a cobalt-free alloy electrode and is similar to that of an electrode containing 10 wt.% cobalt as illustrated in Fig. 11. The $AB_{5+x}$ materials are most interesting as they constitute a new class of compounds which may provide alloys that could be fabricated into low cost, corrosion resistant battery electrodes. The existence of transition metal dumbbells are not unique. They exist in $LaNi_{5+x}$ [55], $RE_2Fe_{17}C_x$, whose $A_2B_{17}$ type structure is an ordered superstructure of $CaCu_5$ lattice, and $AB_7$ compounds where B is Cu or Ni [56,57].

## 11. $AB_2$ hydride electrodes

The active material in these electrodes are Laves phases. These have close packed structures in which the radii of the A and B atoms must lie within a certain range based on a hard sphere packing model. There are three structural types, the hexagonal C14 ($MgZn_2$), the cubic C15 ($MgCu_2$) and the hexagonal C36 ($MgNi_2$). The C14 and C15 structures are common and many form hydride phases [58]. However, the alloys used in battery applications are very complicated and may contain as many as three distinct bulk phases [59]. Ovshinsky et al. [60] describe the properties of a series of alloys containing V, Ti, Zr, Ni, Cr, Co and Fe in various proportions; they qualitatively

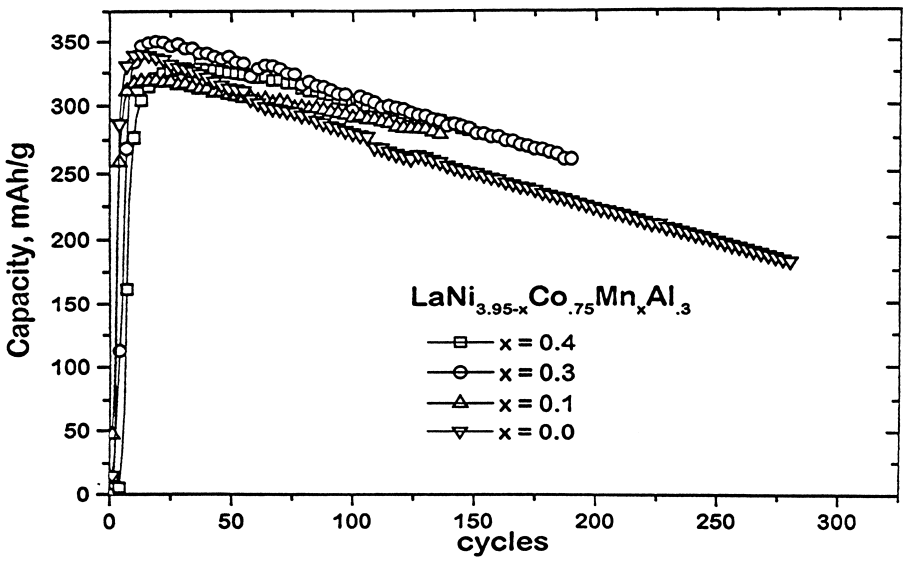


Fig. 9. Charge capacity, $Q$, vs. charge–discharge cycles for $LaNi_{3.95-x}Co_{0.75}Mn_xAl_{0.3}$ electrodes (Ref. [51]).

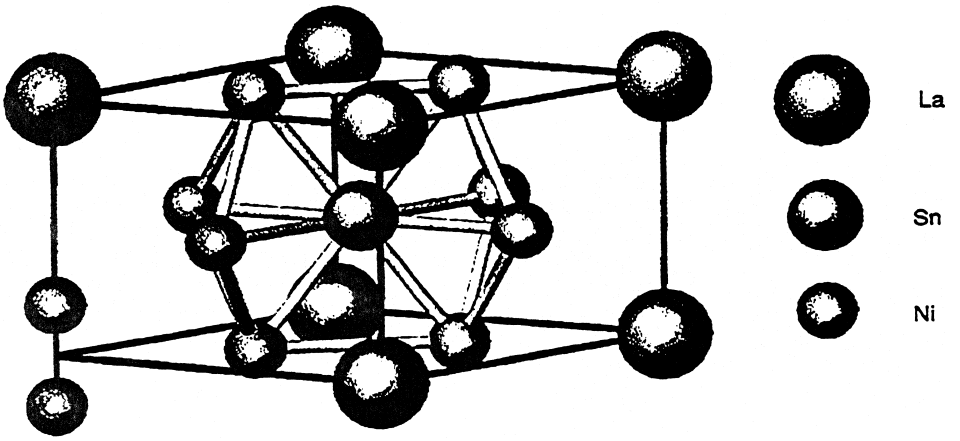


Fig. 10. Schematic representation of super-stoichiometric $AB_{5-x}$ alloys showing B atom dumbbells replacing La on A sites. The P6/mmm space group of the stoichiometric $AB_5$ lattice is preserved (Ref. [54]).

discuss how $AB_2$ alloy properties are influenced by various elemental constituents. Gifford et al. [61] describe an experimental EV battery incorporating an $AB_2$ anode having an energy density of 80 Wh/kg. The battery lost only 18% of its original charge capacity after 800 cycles at 80% depth of discharge.

PCT diagrams of $AB_2$(electrode alloys)/H systems reflect multiphase, non-ideal behavior [60] and PC isotherms are highly sloping with no plateau. However, unlike applications which involve H storage for subsequent use as a gas, battery applications do not require flat, wide plateaus because the pressure is a logarithmic function of the voltage.

The cycle lives of several $AB_2$ electrodes are illustrated in Fig. 12 [62]. In some cases $AB_2$ alloys require many charge–discharge cycles to become fully activated; preactivation via the direct reaction with $H_2$ gas is helpful in this regard. Some pertinent properties and results are given in Table 5. It is of interest to note that $V_H$ in the hydride phase is significantly less than in $AB_5$ hydrides. Consequently, lattice expansion is also significantly reduced. However, the corrosion rates of the electrodes are still appreciable. Indeed for electrode $x=0.25$ the corrosion rate is very high despite a small lattice expansion. Obviously this material is quite sensitive to corrosion and indicates that a moderately high Zr content is necessary to

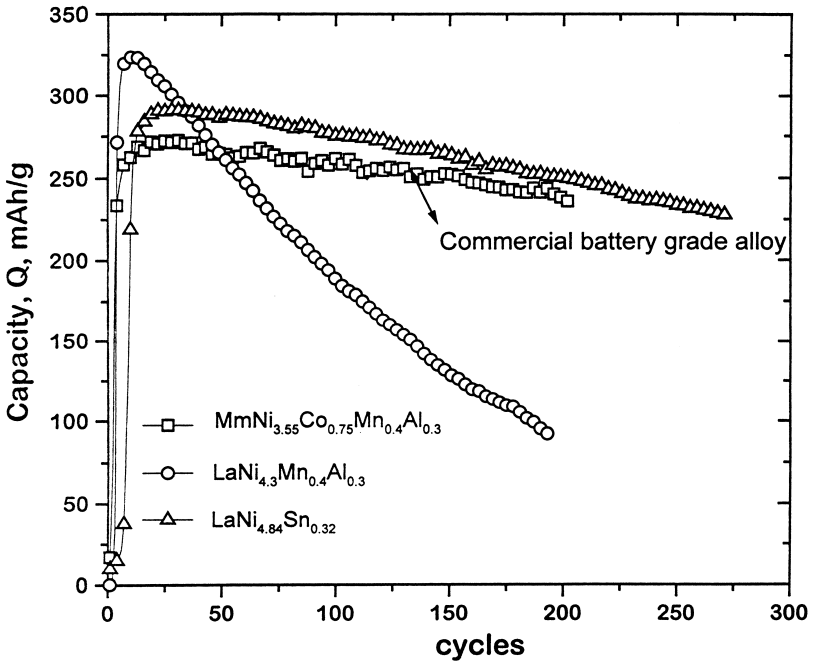


Fig. 11. Charge capacity, *Q*, vs. charge–discharge cycles for electrodes $LaNi_{4.84}Sn_{0.32}$, $LaNi_{4.3}Mn_{0.4}Al_{0.3}$ (also Co-free) and $MmNi_{3.55}Co_{0.75}Mn_{0.4}Al_{0.3}$ (Ref. [53]).

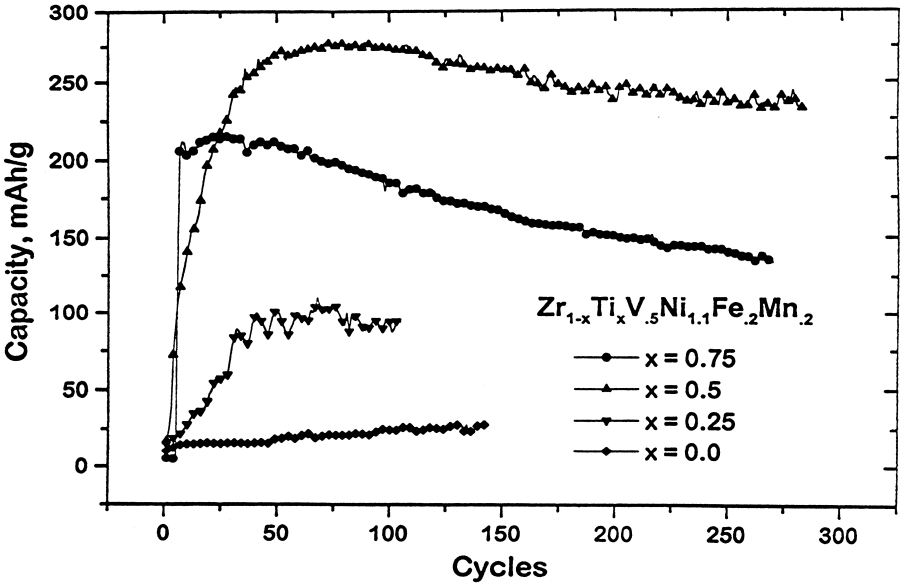


Fig. 12. Charge capacity, $Q$, vs. charge–discharge cycles for $Zr_{1-x}Ti_xV_{0.5}Ni_{1.1}Fe_{0.2}Mn_{0.2}$ electrodes (Ref. [62]).

inhibit corrosion by surface passivation as suggested by Zuttel et al. [63].

## 12. XAS studies of alloy electrode materials

The availability of high intensity, tunable X-rays produced by synchrotron radiation has resulted in the development of new techniques to study both bulk and surface materials properties. Both in situ and ex situ XAS methods have been applied to determine electronic and structural characteristics of electrodes and electrode materials [64,65]. XAS combined with electron yield techniques can be used to distinguish between surface and bulk properties. In the latter procedure X-rays are used to produce high energy Auger electrons [66] which, due to their limited escape depth (≈150–200 Å), can provide information regarding near surface composition.

The element-specific nature of XAS makes it particularly useful for the study of complex $AB_5$ and $AB_2$ metal hydride electrode materials. Mukerjee et al. [46] examined $La_{0.8}Ce_{0.2}Ni_{4.8}Sn_{0.2}$ and $LaNi_{4.8}Sn_{0.2}$ electrodes using in situ XAS. It was determined by analysis of the X-ray absorption near edge structure (XANES) that the presence of Ce reduced Ni corrosion; a finding which confirmed previous cycle life experiments [43]. Tryk et al. have similarly examined $LaNi_5$ [67] and $MmNi_{3.5}Co_{0.8}Mn_{0.3}Al_{0.4}$ [68] electrodes and noted electronic transitions taking place in the metal lattice as a function of charge and the strong interaction of absorbed H with Ni. This is not unexpected as hydrogen occupies a Ni tetrahedral site in $LaNi_5H_6$.

XAS studies have also been carried out on C14 Laves phase alloys, $Ti_{0.5}Zr_{0.5}M_2$ and $Ti_{0.75}Zr_{0.25}M_2$ ($M = V_{0.5}Ni_{1.1}Fe_{0.2}Mn_{0.2}$) [62]. The XANES spectra at the Ni K edge indicates that, unlike the $AB_5$ alloys, there is very little interaction between hydrogen and Ni but rather strong interactions with Ti, V and Zr. The hydrogen is presumably located in tetrahedra that contain large fractions of these three elements whereas the Ni-rich sites are probably empty. Thus, the prime function of Ni in $AB_2$ alloys may be to serve as a catalyst for the electrochemical and hydriding reactions.

Table 5
Effect of Zr in $Ti_{1-x}Zr_xV_{0.5}Ni_{1.1}Fe_{0.2}Mn_{0.2}$ electrodes (Ref. [62])

| $x$ value | $V_H$ Å$^3$ | $Q_{max}$ mAh/g | $n$, H atoms[a] per unit cell | $\%\Delta V/V$ | Corrosion wt.%/cycle |
|---|---|---|---|---|---|
| 0.25 | 1.95 | 215 | 5.48 | 6.45 | 0.214 |
| 0.5 | 2.76 | 299 | 8.12 | 13.1 | 0.097 |
| 0.5 | 2.76 | 278 | 7.56 | 12.3 | 0.083 |
| 0.75 | | 95 | 0.7 | | 0.0 |
| 1.0 | | 27 | 0.2 | | 0.0 |

[a] There are four formula units in the hexagonal C14 unit cell.

## 13. Summary

This survey presents a brief overview of the chemistry of metal–hydrogen systems which are of interest for electrochemical applications. The discussion then focuses on the $AB_5$ class and, to a lesser extent, the $AB_2$ class of metal hydride electrodes. Electrode corrosion is the critical problem associated with the use of metal hydride anodes in batteries. The extent of corrosion is essentially determined by two factors, alloy expansion and contraction in the charge–discharge cycle and chemical surface passivation

via the formation of corrosion resistant oxides or hydroxides. Both factors are sensitive to alloy composition which can be adjusted to produce electrodes having an acceptable cycle life. In complex $AB_5$ alloys the effects of Ce, Co, Mn and Al upon cycle life in commercial type $AB_5$ electrodes are correlated with lattice expansion and charge capacity. XAS results indicate that Ce and Co inhibit corrosion via surface passivation. Cobalt occupies both the midplane and the basal plane in $LaNi(Co, MnAl)_5$ alloys whereas Mn and Al substitute only in the midplane of the $CaCu_5$ structure. The structure of $LaNi_{3.55}Co_{0.75}Mn_{0.33}Al_{0.30}D_x$ remains P6mmm since there is no superlattice formation as in $LaNi_5D_7$ ($P6_3mc$). Non-stoichiometric $La(Ni, Sn)_{5+x}$ alloys were discussed as candidate materials from which low cost, corrosion resistant electrodes may be fabricated.

There are few systematic guidelines which can be used to predict the properties of $AB_2$ metal hydride electrodes. Alloy formulation is primarily an empirical process where the composition is designed to provide a bulk hydride forming phase (or phases) but which will also form a corrosion resistant surface of semi-passivating oxide (hydroxide) layers. Lattice expansion is usually reduced relative to the $AB_5$ hydrides because of a lower $V_H$. Pressure–composition isotherms of complex $AB_2$ electrode materials indicate non-ideal behavior.

Finally, it should be noted that while small Ni–MH batteries are now an article of commerce, a major challenge still remains. It is to produce a low cost $MH_x$ electrode having a long cycle life and a storage capacity of $>300$ mAh/g which would be suitable for use in heavy duty, long life batteries such as those proposed for electric and hybrid vehicles.

## Acknowledgements

The author wishes to acknowledge the support of the DOE Chemical Sciences Division and DOE Office of Transportation Technologies under contract number DE-AC02-98CH10886.

## References

[1] G.D. Sandrock, A panoramic overview of hydrogen storage alloys from a gas reaction point of view, J. Alloys Comp., this volume.
[2] T.B. Flanagan, W.A. Oates, Hydrogen in intermetallic compounds I, in: L. Schlapbach (Ed.), Topics in Applied Physics, Vol. 63, Springer Verlag, New York, 1988, p. 49.
[3] G.G. Libowitz, The Solid State Chemistry of Binary Metal Hydrides, W.A. Benjamin, New York, 1965.
[4] W.M. Mueller, J.P. Blackledge, G.G. Libowitz (Eds.), Metal Hydrides, Academic Press, New York, 1968.
[5] E. Wicke, H. Brodowsky, H. Zuchner, Hydrogen in metals I, in: G. Alefeld, J. Volkl (Eds.), Topics in Applied Physics, Vol. 28, Springer Verlag, New York, 1978, p. 101.
[6] D.N. Gruen, M.H. Mendelsohn, A.E. Dwight, J. Less-Common Metals 63 (1979) 193.
[7] C.E. Lundin, F.E. Lynch, C.B. Magee, J. Less-Common Metals 56 (1977) 19.
[8] D.G. Westlake, J. Less Common Metals 91 (1983) 1.
[9] A.C. Switendick, Z. Physik. Chemie. N.F. 117 (1979) 89.
[10] J.J. Reilly, in: A.F. Andresen, A.J. Maeland (Eds.), Proceedings International Symposium On Hydrides For Energy Storage, Geilo, Norway, Pergamon Press, New York, 1978, p. 301.
[11] J.J. Reilly, Z. Physik. Chemie., N.F. 117 (1979) 155.
[12] J.J. Reilly, R.H. Wiswall, Inorg. Chem. 7 (1968) 2254.
[13] J.J. Reilly, R.H. Wiswall, Inorg. Chem. 13 (1974) 218.
[14] Y. Lei, Y. Wu, Q. Yang, J. Wu, Q. Wang, Z. Physik. Chemie Bd. 183 (1994) S379.
[15] M. Tsukahara, K. Takahashi, T. Mishima, H. Miyamura, T. Sakai, N. Kuriyama, I. Uehara, J. Alloys Comp. 231 (1995) 616.
[16] H.C. Siegmann, L. Schlapbach, C.R. Brundle, Phys. Rev. Lett. 40 (1978) 547.
[17] J.J. Reilly, in: S.L. Holt (Ed.), Inorganic Syntheses, J. Wiley, New York, 1983, p. 90.
[18] E.W. Justi, H.H. Ewe, H. Stephan, Energy Conversion 13 (1973) 109.
[19] A. Percheron-Guegan, J.C. Achard, J. Sarradin, G. Bronoel, in: A.F. Andresen, A.J. Maeland (Eds.), Proceedings International Symposium On Hydrides For Energy Storage, Geilo, Norway, Pergamon Press, New York, 1978, p. 485.
[20] M.H.J. Van Rikswick, in: A.F. Andresen, A.J. Maeland (Eds.), Proceedings International Symposium On Hydrides For Energy Storage, Geilo, Norway, Pergamon Press, New York, 1978, p. 261.
[21] J.J.G. Willems, Philips J. Res. 39 (Suppl. 1) (1984).
[22] M. Ikowa, H. Kawano, I. Matsumoto, N. Yanagihara, Eur. Patent Appl. #0271043 (1987).
[23] H. Ogawa, M. Ikowa, H. Kawano, I. Matsumoto, Power Sources 12 (1988) 393.
[24] M. Ikoma, S. Hamada, N. Morishita, Y. Hoshina, K. Ohta, T. Kimura, in: P.D. Bennett, T. Sakai (Eds.), Proceedings of the Symposium On Hydrogen and Metal Hydride Batteries, Vol. 94-2, The Electrochemical Society, Pennington NJ, 1994, p. 370.
[25] J.H.N. van Vucht, F.A. Kuipers, H.C.A.M. Bruning, Philips Res. Rep. 25 (1970) 133.
[26] K.H.J. Buschow, A.R. Medima, in: A.F. Andresen, A.J. Maeland (Eds.), Proceedings International Symposium On Hydrides For Energy Storage, Geilo, Norway, Pergamon Press, New York, 1978, p. 235.
[27] S.W. Lambert, D. Chandra, W.N. Cathey, F.E. Lynch, R.C. Bowman Jr., J. Alloys Comp. 187 (1992) 113.
[28] P.D. Goodell, P.S. Rudman, J. Less-Common Metals 89 (1983) 117.
[29] J.J. Reilly, Y. Josephy, J.R. Johnson, Z. Physik. Chemie. N.F. 164 (1989) S1241.
[30] M. Miyamoto, K. Yamaji, Y. Nakata, J. Less Common Metals 89 (1989) 111.
[31] J.J. Reilly, R.H. Wiswall Jr., Hydrogen Storage and Purification Systems, US Atomic Energy Commission, Brookhaven National Laboratory, Upton NY 11973, 1972, BNL-17 136.
[32] M. Latroche, J. Rodriguez-Carvajal, A. Pecheron-Guegan, F. Bouree-Vigneron, J. Alloys Comp. 18 (1995) 64.
[33] T. Vogt, J.J. Reilly, J.R. Johnson, G.D. Adzic, J. McBreen, J. Electrochem. Soc. 146 (1999).
[34] P. Thompson, J.J. Reilly, L.M. Corliss, J.M. Hastings, R. Hempelmann empe, J. Phys. F., Metal Phys. 16 (1986) 679.
[35] C. Lartigue, A. Percheron-Guegan, J.C. Achard, J.L. Soubeyoux, J. Less Common Metals 113 (1985) 127.
[36] T. Sakai, H. Yoshinaga, H. Miyamura, N. Kuriyama, H. Ishikawa, J. Alloys Comp. 180 (1992) 37.
[37] A. Percheron-Guegan, J.-M. Welter, Hydrogen in intermetallic compounds I, in: L. Schlapbach (Ed.), Topics in Applied Physics, Vol. 63, Springer Verlag, New York, 1988, p. 11.

[38] K. Petrov, A.A. Rostami, A. Visintin, S. Srinivasan, J. Electrochem. Soc. 141 (1994) 1747.
[39] G.D. Adzic, J.R. Johnson, S. Mukerjee, J. McBreen, J.J. Reilly, in: Meeting Abstracts of the 189th Meeting of the Electrochemical Society, Los Angeles, Vol. 96-1, The Electrochemical Society, Pennington NJ, 1996, Abstract #65.
[40] J.J.G. Willems, K.H.J. Buschow, J. Less-Common Metals 129 (1987) 13.
[41] M. Latroche, A. Percheron-Guegan, Y. Chabre, J. Bouet, J. Pannetier, E. Ressouche, J. Alloys Comp. 231 (1995) 537.
[42] G. Adzic, J.R. Johnson, S. Mukeijee, J. McBreen, J.J. Reilly, J. Alloys Comp. 253/254 (1997) 579.
[43] G. Adzic, J.R. Johnson, J.J. Reilly, J. McBreen, S. Mukerjee, M.P.S. Kumar, W. Zhang, S. Srinivasan, J. Electrochem. Soc. 142 (1995) 3429.
[44] T. Sakai, T. Hazama, H. Miyamura, N. Kuriyama, A. Kato, H. Ishikawa, J. Less-Common Metals 172–174 (1991) 1175.
[45] A.J. Davenport, H.S. Isaacs, M.W. Kendig, Corrosion Sci. 32 (5/6) (1991) 653.
[46] S. Mukerjee, J. McBreen, J.J. Reilly, J.R. Johnson, G. Adzic, K. Petrov, M.P.S. Kumar, W. Zhang, S.J. Srinivasan, J. Electrochem. Soc. 142 (1995) 2278.
[47] T. Sakai, K. Oguro, H. Miyamura, N. Kuriyama, A. Kato, H. Ishikawa et al., J. Less-Common Metals 161 (1990) 193.
[48] M. Kanda, M. Yamamoto, K. Kanno, Y. Satoh, H. Hayashida, M. Suzuki, J. Less-Common Metals 129 (1987) 13.
[49] S. Mukerjee, J. McBreen, G.D. Adzic, J.R. Johnson, J.J. Reilly, The function of cobalt in $AB_5H_x$ metal hydride electrodes as determined by X-ray absorption spectroscopy, in: Extended Abstracts, National Meeting of the Electrochemical Society, San Antonio, Texas USA, October, Vol. 96-2, 1996, Abstract #48.
[50] T. Sakai, H. Miyamura, H. Kuriyama, A. Kato, K. Oguro, H. Ishikawa, J. Less Common Metals 159 (1990) 127.
[51] G. Adzic, J.R. Johnson, S. Mukerjee, J. McBreen, J.J. Reilly, in: W.A. Adams, A.R. Landgrebe, R. Scrosati (Eds.), Symposium Proceedings of Exploratory Research and Development of Batteries For Electric and Hybrid Vehicles, Vol. 96-14, Electrochemical Society, Pennington NJ, USA, 1996, p. 189.
[52] P.H.L. Notten, R.E.F. Einerhand, J.L.C. Daams, J. Alloys Comp. 210 (1994) 221.
[53] P.H.L. Notten, R.E.F. Einerhand, J.L.C. Daams, J. Alloys Comp. 210 (1994) 233.
[54] T. Vogt, J.J. Reilly, J.R. Johnson, G.D. Adzic, J. McBreen, Electrochem. Solid State Lett. 2 (1999) 111.
[55] K.H.J. Buschow, H.H. Van Mal, J. Less-Common Metals 29 (1972) 203.
[56] W. Coene, F. Hakkens, T.H. Jacobs, K.H.J. Buschow, J. Solid State Chem. 92 (1991) 191.
[57] D. Givord, R. Lemaire, J.M. Moreau, E. Roudaut, J. Less-Common Metals 29 (1972) 361.
[58] D.G. Ivey, D.O. Northwood, Z. Phys. Chem. N.F. 147 (1986) 191.
[59] J. Huot, E. Akiba, Y. Ishido, J. Alloys Comp. 231 (1995) 85.
[60] S.R. Ovshinsky, M.A. Fetcenko, J. Ross, Science 260 (1993) 176.
[61] P.R. Gifford, M.A. Fetcenko, S. Venkatesan, D.A. Corrigan, A. Holland, S.K. Dhar, S.R. Ovshinsky, in: P.D. Bennett, T. Sakai (Eds.), Proceedings of the Symposium On Hydrogen and Metal Hydride Batteries, Vol. 94-27, The Electrochemical Society, Pennington NJ, 1996, p. 353.
[62] J.R. Johnson, S. Mukerjee, G.D. Adzic, J.J. Reilly, J. McBreen, In situ XAS studies on $AB_2$ type metal hydride alloys for battery applications, in: Presented at the International Symposium On Metal Hydrogen Systems; Fundamentals and Applications. Les Diablerers, Switzerland, August, 1996.
[63] A. Zuttel, F. Meli, L. Schlapbach, J. Alloys Comp. 231 (1995) 645.
[64] J. McBreen, X-ray absorption studies of battery materials, in: W.A. Adams, A.R. Landgrebe, R. Scrosati (Eds.), Symposium Proceedings of Exploratory Research and Development of Batteries For Electric and Hybrid Vehicles, Vol. 96-14, Electrochemical Society, Pennington NJ, USA, 1996, p. 162.
[65] D.A. Scherson, Interface, Fall S. #3 (1996) 34.
[66] A.N. Mansour, C.A. Melandres, S.J. Poon, Y. He, G.J. Shiflet, J. Electrochem. Soc. 143 (1987) 219.
[67] D.A. Tryk, I.T. Bae, Y. Hu, S. Kim, M.R. Antonio, D.A. Sherson, J. Electrochem. Soc. 142 (3) (1995) 824.
[68] D.A. Tryk, I.T. Bae, D.A. Sherson, M.R. Antonio, G.W. Jordan, E.L. Huston, J. Electrochem. Soc. 142 (5) (1995) L76.